Journal of the Korean Society for Nondestructive Testing
Vol. 27, No. 6 (2007. 12)

Nonlinear Displacement Discontinuity Model for Generalized Rayleigh Wave in Contact Interface

Nohyu Kim*,† and Seungyong Yang**

Abstract Imperfectly jointed interface serves as mechanical waveguide for elastic waves and gives rise to two distinct kinds of guided wave propagating along the interface. Contact acoustic nonlinearity (CAN) is known to plays major role in the generation of these interface waves called generalized Rayleigh waves in non-welded interface. Closed crack is modeled as non-welded interface that has nonlinear discontinuity condition in displacement across its boundary. Mathematical analysis of boundary conditions and wave equation is conducted to investigate the dispersive characteristics of the interface waves. Existence of the generalized Rayleigh wave(interface wave) in nonlinear contact interface is verified in theory where the dispersion equation for the interface wave is formulated and analyzed. It reveals that the interface waves have two distinct modes and that the phase velocity of anti-symmetric wave mode is highly dependent on contact conditions represented by linear and nonlinear dimensionless specific stiffness.

Keywords: Generalized Rayleigh Wave, Contact Nonlinearity, Dispersion, Interface Wave

1. Introduction

Contact-type discontinuity such as closed cracks leads to an anomalously high level of nonlinearity. Well-known acoustical manifestation of the nonlinear behavior is the generation of its harmonics. In particular, the transmission and reflection characteristics at contacting surfaces have been the subject of extensive research relating to the evaluation of contact interfaces and integrity monitoring in NDT. However, practical implementation of the second harmonic method requires lots of efforts to minimize nonlinear distortions in transmitting/receiving devices. The physical nature of the contact acoustic nonlinearity(CAN) has been explained by developing several mathematical models of contact-type interface(Biwa et al., 2005; S. Roy et al., 1995). From their works, the variation of contact area within the interface due to deformation of asperities is known to cause nonlinear elasticity of the interface. This interface is considered as a linear spring whose stiffness is proportional to the contact area within the interface. The linear model of the spring-type crack interface connects displacements with stresses on both sides of the interface by employing spring stiffness. Theoretically, the transmission/reflection spectra of the normally incident longitudinal and shear waves are governed by the normal and tangential stiffnesses of the contact interface respectively. These interfacial stiffnesses are known to offer useful information on the nature of the contact interface. In addition to the transmission/reflection characteristics, the interfacial stiffnesses can be

Received: November 15, 2007, Accepted: December 11, 2007. * Department of Mechatronic Engineering, Korea University of Technology and Education 307 Gajun-Ri, Byungchun-Myun, Chunan 330-860, Korea, ** Department of Mechanical Engineering, Korea University of Technology and Education 307 Gajun-Ri, Byungchun-Myun, Chunan 330-860, Korea, † Corresponding author: nykim@kut.ac.kr

evaluated by elastic waves propagating along the contact interface, as has been explored by several researchers (Biwa, 2006 and Pyrak-Nolte, 1987 and 1992). They have carried out theoretical analysis of the steady-state wave propagation along a spring-type interface between two elastic half-spaces and shown the existence of two distinct modes of propagation; namely, the symmetric mode and the anti-symmetric mode that are governed separately by the normal and the tangential interfacial stiffnesses. These waves are a special kind of guided waves in the interface and not Stonely waves but because the material property of the half spaces of each side of interface are same. These wave modes propagating along the interface can be quite useful to detect surface breaking cracks which are closed so tightly that they do not produce linear scattering waves during reflection/transmission of linear ultrasound.

In this paper, a hysteretic nonlinear displacement discontinuity model for the non-welded contact interface is sought and analyzed to investigate the possibility for interface waves to propagate along the nonlinear contact boundaries and to estimate contact state of the interface. Dispersion equation of the waves is derived by combining the wave equation with the boundary conditions: nonlinear discontinuous displacements. In the model, the traction applied to the interface is defined to be hysteretic to the discontinuity in displacement using the nonlinear specific stiffness of the contact interface. The existence of the waves is verified in theory by plane wave analysis along the contact interface.

2. Nonlinear Displacement Discontinuity Model for Contact Interface

Closed cracks in solid medium represent mechanical discontinuity that strongly affects the propagation of elastic waves either across or along the crack boundary. At the micro-scale, the contact interface appears as two surfaces of irregular topology which intersect to form micro-void spaces and asperities of contact. The presence of the asperities and voids within planar crack define a thin, compliant zone with effective normal and shear stiffnesses that can range from near zero for open crack to almost infinite values for completely closed crack which are bonded or subjected to high compressive stresses. Typically a crack loaded in shear or compression exhibits a highly nonlinear stress-displacement relationship resulting from deformation of the asperities, the number and distribution of which changes with load as shown in Fig. 1(a). Hysterisis also appears often in the stress-displacement curve in Fig. 1(a) during the loading and unloading (Kim, et al, 2004 and 2006), indicating the presence of inelastic deformation of the asperities of contact and frictional sliding between contacts. Those

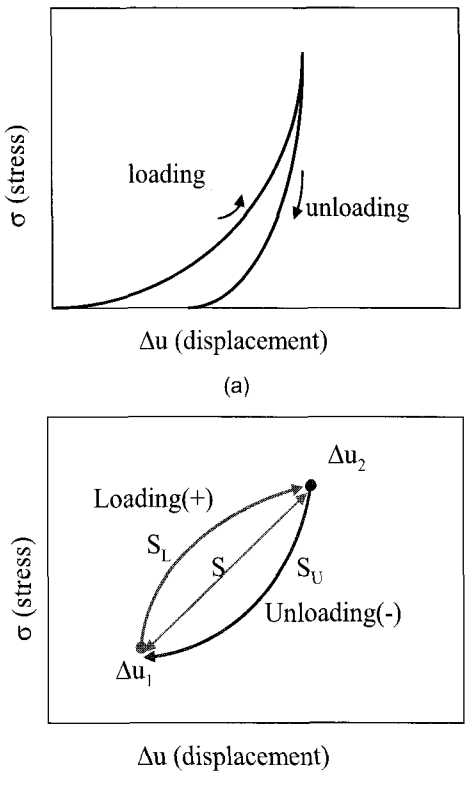

Fig. 1 Hysteretic nonlinear behavior of contact interface, (a) loading-unloading curves, (b) idealized hysteresis

features of closed cracks play an important role in the amplitudes, phases, and velocities of elastic waves. Specific stiffness is the quantity that relates the displacement to the traction of closed contact interface, which may be linear or nonlinear. In linear displacement discontinuity model or imperfect interface model (Pyrak-Nolte and Cook, 1992), two contact surfaces of each boundary are assumed to be continuous in stress but not in displacement at which the specific stiffness is defined as a linear spring such that the stress is proportional to the displacement difference.

Let's consider a nonlinear hysteretic-oscillatory deformation cycle $S_L - S_U$ between two deformation states, Δu_1 and Δu_2 in Fig. 1(b) caused by acoustic wave. The irreversible deformation starts from Δu_1 to Δu_2 following the loading curve S_L and returns to the original point u_1 via the unloading curve S_L completing the one cycle of motion. A linear deformation path S from Δu_1 to Δu_2 is also presented in Fig. 1(b) to introduce the linear stiffness κ from the proportional linearity. During the loading process S_L of the hysteresis cycle, the work done to the medium by stress is larger than the linear case, while the work done by the medium during the unloading process S_U is smaller than the linear unloading. The amount of the energy difference is dissipated by the nonlinearity and hysteresis of contact interface. In this processes, the contact interface works as a nonlinear spring that gets stiffer during the loading and softer for unloading. Thus the nonlinear spring can be formulated by adding some stiffness to the linear spring during the loading and subtracting the same stiffness from the linear spring during unloading. Controlling the spring stiffness during the cycle produces an irreversible forces in the spring such as Coulomb friction force and/or viscous force. Then the stiffness is defined as the nonlinear stiffness κ_n. The nonlinear stiffness κ_n is complex in general and can be determined by the energy dissipation produced by the corresponding nonlinear process S_U or S_L. Based on the above assumptions, the stress-displacement relationship across the interface is expressed by the superposition of linear spring κ and nonlinear hysteretic spring κ_n such as

$$\begin{aligned}
\sigma_{loading} &= \kappa_{loading}(\Delta u)^a \\
&= \kappa\,(\Delta u_2 - \Delta u_1) + \kappa_n(\Delta u_2 - \Delta u_1) \\
&\qquad \text{for } S_L(loading) \\
\sigma_{unloading} &= \kappa_{unloading}(\Delta u)^b \\
&= \kappa\,(\Delta u_2 - \Delta u_1) - \kappa_n(\Delta u_2 - \Delta u_1) \\
&\qquad \text{for } S_U(unloading)
\end{aligned} \tag{1}$$

where a and b are power indices for nonlinearity related with the loading and unloading. Now suppose that two elastic bodies with identical material properties which are put into contact by static pressure. Due to the surface roughness, the contact at the interface forms a microscopically imperfect elastic-plastic deformation between the upper (denoted by superscript u) and lower (denoted by superscript l) rough surfaces as shown in Fig. 2. The displacement of the upper surface is $\boldsymbol{u}^u = (u_x^u, u_z^u)$ and the lower surface $\boldsymbol{u}^l = (u_x^l, u_z^l)$. The sizes of asperities are assumed to be much smaller than the wavelength of acoustic wave so that the incoherent scattering from the interface is negligible. Since both displacement and stress have discontinuity across the interface, some

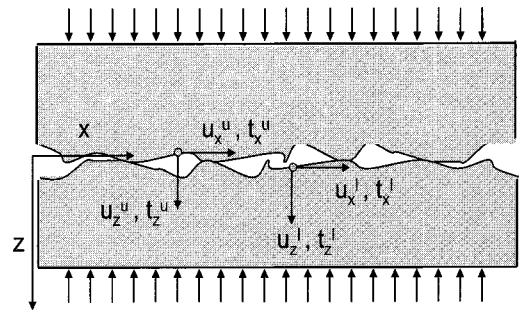

Fig. 2 Two surfaces in contact by pressure

boundary conditions are necessary to connect those discontinuities. These conditions are obtained from the constitutive properties of the interface formulated by the hysteretic nonlinear spring κ_n in eqn. (1) between the tractions and the displacement across and along the interface in normal and shear directions (z and x in Fig. 2). The stress-displacement relations given by eqn. (1) are adopted and applied to the interface of Fig. 2 resulting in the following equations

$$\begin{aligned} t_x^u &= \kappa_x(\Delta u_x) + \kappa_{nx}(\Delta u_x) \\ &= \kappa_x(u_x^u - u_x^l) + \kappa_{nx}(u_x^u - u_x^l) \\ t_x^l &= \kappa_x(\Delta u_x) - \kappa_{nx}(\Delta u_x) \\ &= \kappa_x(u_x^u - u_x^l) - \kappa_{nx}(u_x^u - u_x^l) \\ t_z^u &= \kappa_z(\Delta u_z) + \kappa_{nz}(\Delta u_z) \\ &= \kappa_z(u_z^u - u_z^l) + \kappa_{nz}(u_z^u - u_z^l) \\ t_z^l &= \kappa_z(\Delta u_z) - \kappa_{nz}(\Delta u_z) \\ &= \kappa_z(u_z^u - u_z^l) - \kappa_{nz}(u_z^u - u_z^l) \end{aligned} \tag{2}$$

where, t_x^u ,t_x^l ,t_z^u ,t_z^l are the normal and shear tractions on the upper and lower surface, κ_z ,κ_x are the linear normal and shear stiffness, and κ_{nx} ,κ_{nz} nonlinear normal and shear stiffness, and u_x^u ,u_x^l ,u_z^u ,u_z^l are the displacements of the upper and lower surface in x and z as shown in Fig. 2. The positive and negative sign of the nonlinear stiffnesses in eqn. (2) represent the loading and unloading state of the tractions according to the relative displacement of the lower and upper surfaces in Fig. 2. The sign is assigned positive if the displacement and traction increase with the coordinate x and z, and negative if the displacement and traction decrease with the coordinate x and z. It is clear from this sign rule that the displacements and tractions of the lower surface are larger than those of the upper surface in the coordinate system of Fig. 2. Thus the traction on the lower surface of Fig. 2 acts as the unloading process of the hysteresis defined in Fig. 1 with respect to those of the upper surface. It could be possible to use the sign rule conversely. It has been demonstrated by other researches (Nihei, et al, 1995) that the dynamic stiffness in eqn. (2) is independent of wave frequency in case of relatively large wavelength compared with the asperities of contact, and well defined as static stiffness that can be obtained from the stress-displacement curve such as Fig. 1. It can be found from eqn. (2) that if the nonlinear stiffnesses κ_{nx} ,κ_{nz} are all zero, eqn. (2) leads to $t_x^u = t_x^l$, $t_z^u = t_z^l$, which means stress continuity across the interface. It becomes the same boundary condition as the displacement discontinuity model (Pyrak-Nolte et al., 1987). It also represents the limiting cases for a traction-free boundary condition as κ_x and κ_z go to zero and for a welded interface as κ_x and κ_z become infinity. Equation (2) gives a simple but pertinent model for the nonlinear properties of a non-welded contact between two identical media.

3. Existence of Guided Waves in Contact Interface

The existence of guided waves propagating along the contact interface in the form of interface waves or generalized Rayleigh waves is found and derived by linear modeling of the contact as a non-welded interface in the studies on fractures (Biwa et al., 2005; Delsanto et al., 2002; Pyrak-Nolte et al., 1987). Non-welded interface is described in the linear models by a set of boundary conditions: stress across the interface is continuous but the displacements across or along the interface are discontinuous having linear relation with the stress. This displacement discontinuity boundary condition is formulated by adopting the linear specific stiffnesses connecting the displacement discontinuity to the traction of contact interface.

In this work, the plane wave analysis is made similarly based on this basic concept but with nonlinear displacement discontinuity model introduced in eqn. (2) of previous section to

investigate the existence and characteristics of nonlinear guided waves(interface wave) in the contact interface. Generalized Rayleigh wave in interface is a special form of guided wave that propagates along the boundary between two identical media unlike the Stoneley waves in two different media. Trapped Rayleigh waves are localized in the interface within a zone that may extend only a few wavelengths away from the boundary, allowing these waves to travel large distance while suffering little reduction in amplitude. The displacement vector for an inhomogeneous plane wave propagating along the contact interface in x direction with the amplitude that decays exponentially with distance z away from the interface can be expressed for the upper medium using the superscript u as (Nihei et al., 1995)

$$u_x^u(x,z) = \omega[i\frac{A_1}{c}e^{-p\omega z} + qB_1e^{-q\omega z}]e^{i(\kappa x-\omega t)}$$
$$u_z^u(x,z) = \omega[-pA_1e^{-p\omega z} + i\frac{B_1}{c}e^{-q\omega z}]e^{i(\kappa x-\omega t)} \quad (3)$$

and for the lower medium using the superscript l

$$u_x^l(x,z) = \omega[i\frac{A_2}{c}e^{+p\omega z} - qB_2e^{+q\omega z}]e^{i(\kappa x-\omega t)}$$
$$u_z^l(x,z) = \omega[pA_2e^{+p\omega z} + i\frac{B_2}{c}e^{+q\omega z}]e^{i(\kappa x-\omega t)} \quad (4)$$

where, ω is the angular frequency, t is time, A_1, A_2, B_1 and B_2 are unknown constants, c is the phase velocity of the inhomogeneous wave, and p and q are wave numbers given by

$$p = \sqrt{\frac{1}{c^2} - \frac{1}{c_p^2}}\ ,\ q = \sqrt{\frac{1}{c^2} - \frac{1}{c_s^2}} \quad (5)$$

where, c_p and c_s are the compressional and shear wave velocity respectively. Tractions in the upper and lower medium obtained by substituting eqns. (3) and (4) into Hooke's law are written by

$$t_x^u(x,z) = \omega^2[-2ip\mu\frac{A_1}{c}e^{-p\omega z} - \mu NB_1e^{-q\omega z}]e^{i(\kappa x-\omega t)}$$
$$t_z^u(x,z) = \omega^2[(Lp^2 - \frac{\lambda}{c^2})A_1e^{-p\omega z} - 2i\mu q\frac{B_1}{c}e^{-q\omega z}]e^{i(\kappa x-\omega t)}$$
$$t_x^l(x,z) = -\omega^2[2ip\mu\frac{A_2}{c}e^{+p\omega z} - \mu NB_2e^{+q\omega z}]e^{i(\kappa x-\omega t)} \quad (6)$$
$$t_z^l(x,z) = -\omega^2[(Lp^2 - \frac{\lambda}{c^2})A_2e^{+p\omega z} + 2i\mu q\frac{B_2}{c}e^{+q\omega z}]e^{i(\kappa x-\omega t)}$$

where, λ and μ are Lame's constants, $L = (\lambda + 2\mu)$ and $N = (c^{-2} + q^2)$. Substituting eqns. (3), (4) and (6) into the nonlinear displacement discontinuity condition given by eqn. (2) yields a system of four homogeneous linear equations for four undetermined constants, A_1, A_2, B_1 and B_2. From the necessary condition for the existence of a non-trivial solution of the linear equations, the determinant of the coefficient matrix vanishes, which is given by

$$\begin{vmatrix} \frac{i}{c}(2\kappa_z + 2\mu\omega p) & (2q\kappa_x + \mu\omega N) & -\frac{i}{c}(2\kappa_x + 2\mu\omega p) & (2q\kappa_x + \mu\omega N) \\ (2p\kappa_z - \omega Q) & -\frac{i}{c}(2\kappa_z + 2\mu\omega q) & (2p\kappa_z - \omega Q) & \frac{i}{c}(2\kappa_z + 2\mu\omega q) \\ \frac{i}{c}(2\kappa_{nx} + 2\mu\omega p) & (2q\kappa_{nx} + \mu\omega N) & -\frac{i}{c}(2\kappa_{nx} - 2\mu\omega p) & (2q\kappa_{nx} - \mu\omega N) \\ (2p\kappa_{nz} - \omega Q) & -\frac{i}{c}(2\kappa_{nz} + 2\mu\omega q) & (2p\kappa_{nz} + \omega Q) & \frac{i}{c}(2\kappa_{nz} - 2\mu\omega q) \end{vmatrix} = 0 \quad (7)$$

where, $Q = (\lambda c^{-2} - Lp^2)$. Examining the first two equations of eqn. (7) reveals that only two combinations of solutions are possible corresponding to:

i) $A_2 = -A_1\ ,\ B_2 = B_1$ (8)

ii) $A_2 = A_1\ ,\ B_2 = -B_1$ (9)

Replacing A_1, B_2 with A_1, B_1 in eqn. (7) using eqns. (8) and (9) produces two wave motions, one is symmetric about interface, and the other is anti-symmetric about the interface. For the conditions $A_2 = -A_1$, $B_2 = B_1$ provoking the anti-symmetric motion, the determinant in

eqn. (7) reduces to

$$c_s^4[\frac{4pq}{c^2}+N\frac{Q}{\mu}]+\frac{\kappa_x}{\mu\omega}\cdot 2qc_s^2+\frac{\kappa_{nx}}{\mu\omega}\frac{2i}{c}c_s^4[2pq-N]=0 \quad (10)$$

Substituting the definitions of N, Q, p, and q into eqn. (10) and rewriting it with dimensionless quantities gives the dispersion equation for anti-symmetric motion in nonlinear contact interface in more concise expression.

$$[4\alpha^2\sqrt{\alpha^2-1}\cdot\sqrt{\alpha^2-\beta^2}-(1-2\alpha^2)^2]+2(\frac{\kappa_x}{\omega Z_s})\sqrt{\alpha^2-1}+2i(\frac{\kappa_{nx}}{\omega Z_s})\alpha[1-2\alpha^2+2\sqrt{\alpha^2-1}\cdot\sqrt{\alpha^2-\beta^2}]=0 \quad (11)$$

where, $\alpha=\frac{c_s}{c}$, $\beta=\frac{c_s}{c_p}$, $Z_s=\rho c_s$ is the shear acoustic impedance of the medium and $\frac{\kappa_x}{\omega Z_s}$, $\frac{\kappa_{nx}}{\omega Z_s}$ are the linear and nonlinear specific shear stiffnesses. In the same manner, the dispersion equation for symmetric wave motion of nonlinear contact interface is obtained by substituting eqn. (9) into eqn. (7). For the symmetric motion, $A_2=A_1$, $B_2=-B_1$, eqn. (7) is written by

$$(2p\kappa_z-\omega Q)(-\frac{2i}{c}\kappa_{nz}+\mu\omega N)+\frac{i}{c}(2\kappa_z+2\mu\omega q)(2p\kappa_{nz}+\frac{2i}{c}\mu\omega p)=0 \quad (12)$$

or

$$\mu\omega[QN+\frac{4}{c^2}\mu pq]+\kappa_z\cdot 2p\mu-\kappa_{nz}\cdot\frac{2i\mu}{c}[2pq+\frac{Q}{\mu}]=0$$

Thus, the dispersion equation for symmetric motion can be represented in terms of the ratios of acoustic velocities, α and β, as follows

$$[4\alpha^2\sqrt{\alpha^2-1}\cdot\sqrt{\alpha^2-\beta^2}-(1-2\alpha^2)^2]+2(\frac{\kappa_z}{\omega Z_s})\sqrt{\alpha^2-\beta^2}+2i(\frac{\kappa_{nz}}{\omega Z_s})\alpha[1-2\alpha^2+2\sqrt{\alpha^2-1}\cdot\sqrt{\alpha^2-\beta^2}]=0 \quad (13)$$

where, $\frac{\kappa_z}{\omega Z_s}$, $\frac{\kappa_{nz}}{\omega Z_s}$ are linear and nonlinear specific normal stiffnesses. Eqns. (11) and (13) are the complete dispersion equations describing the interface waves propagating along the nonlinear contact interface. It is clear that the first terms of eqns. (11) and (13) represent the free Rayleigh equation for the free boundary condition. Second and third terms of eqns. (11) and (13) result from the linear and nonlinear contact of interface surfaces, respectively. Eqn. (11) and (13) include the angular frequency ω, which means that the waves are dispersive, so that the wave velocities vary with the frequency as well as material properties such as contact stiffnesses. The symmetric and anti-symmetric waves represented by eqns. (11) and (13) are generalized Rayleigh waves, which can be schematized in Fig. 1. They degenerate to the Rayleigh waves on the free surface when the dimensionless linear and nonlinear interface stiffnesses are set to zero. If they are finite, eqns. (10) and (11) unlike the Rayleigh equation become dispersive. Both waves have prograde particle motion and the symmetric wave mode is faster than the anti-symmetric wave. Eqns. (11) and (13) also show that the symmetric wave mode comes from the normal coupling between the surfaces of the interface and the anti-symmetric wave from the tangential shear coupling.

In order for the interface waves to exist and propagate, eqns. (11) and (13) should have real roots. However, the symmetric wave motion of

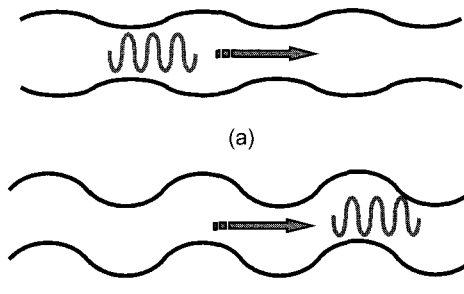

Fig. 3 Generalized Rayleigh waves, (a) symmetric mode, (b) anti-symmetric mode

eqn. (13) don't have real roots at all regardless of the linear and nonlinear stiffnesses except that the nonlinear stiffness is zero. Therefore the symmetric wave does not exist all the time. From eqn. (11) it is obvious too that the ant-symmetric wave have real roots only if the nonlinear stiffness is pure imaginary complex, i.e. $\kappa_{nx} = i\eta(\eta$ is real number). Otherwise the wave motions exist only as leaky waves with energy loss through the acoustic radiation. For instance, if the interface boundary behaves like viscous damper, the equations have real roots and the waves propagate along the interface without big energy loss.

However, if nonlinear effect is very small and negligible, the dispersion equation for symmetric waves is simplified by setting $\kappa_{nx} = 0$,

$$[4\alpha^2\sqrt{\alpha^2-1}\cdot\sqrt{\alpha^2-\beta^2}-(1-2\alpha^2)^2]+ 2(\frac{\kappa_z}{\omega Z_s})\sqrt{\alpha^2-\beta^2}=0 \quad (14)$$

Similarly, the dispersion equation of anti-symmetric wave motion is obtained by substituting eqn. (8) into eqn. (7) when $\kappa_{nx} = 0$,

$$[4\alpha^2\sqrt{\alpha^2-1}\cdot\sqrt{\alpha^2-\beta^2}-(1-2\alpha^2)^2]+ 2(\frac{\kappa_x}{\omega Z_s})\sqrt{\alpha^2-1}=0 \quad (15)$$

Eqns. (14) and (15) are exactly same as the dispersion equation for the linear displacement discontinuity model developed by Pyrak-Nolte and Cook, 1992. If the interface is free of stress, i.e., $\kappa_x = \kappa_{nx} = \kappa_{nz} = \kappa_{nz} = 0$, eqns. (17) and (18) lead to the famous Rayleigh characteristic equation for free surface.

$$4\alpha^2\sqrt{\alpha^2-\beta^2}\sqrt{\alpha^2-1}-(1-2\alpha^2)^2=0 \quad (16)$$

The symmetric wave given by eqn. (15) has complex roots when $(\frac{\kappa_z}{\omega Z_s}) < (\frac{\kappa_z}{\omega Z_s})_{cr} = 2\sqrt{2(1-\nu)}$, and decays into medium exponentially as leaky wave even though the nonlinear stiffness is zero. Contrarily the anti-symmetric wave of eqn. (15) always has real roots and exists for all possible stiffness values and frequencies. Because of this useful feature of the anti-symmetric wave (A-wave), the study is focused on the A-waves excluding the symmetric wave hereafter.

4. Dispersion of Anti-Symmetric Waves in Contact Interface

Fig. 4 depicts the dispersion curves of the interface wave (anti-symmetric mode) for three values of linear stiffness as a function of the nonlinear stiffness. Clearly observed in Fig. 4 is the monotonous increase of the phase velocity ratio, $\alpha = c_s/c$(decrease of the phase velocity), with the increase of the nonlinear stiffness κ_{nx}. Even when the nonlinear stiffness is less than $i\kappa_{nx}/\omega Z_s = 0.1$, the phase velocity decreases significantly with the increase of the nonlinear stiffness. In the limiting case that the nonlinear stiffness $\frac{i\kappa_{nx}}{\omega Z_s}$ approaches 0.5 in Fig. 4, the phase velocity of interface wave asymptotes to the Rayleigh wave velocity regardless of the linear stiffness and material properties. No propagating waves exist beyond the value of $\kappa_{nx}/\omega Z_s$=0.5 as shown in Fig. 4, where the phase velocity of the anti-symmetric interface

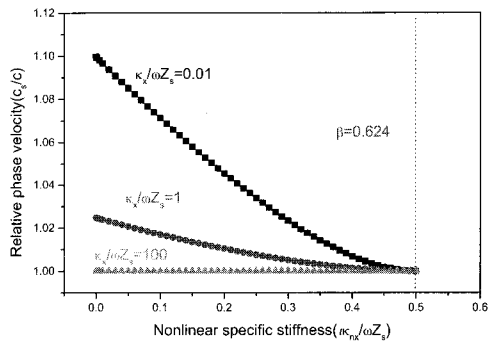

Fig. 4 Phase velocity variation of A-wave with respective to the nonlinear specific stiffness $\frac{\kappa_{nx}}{\omega Z_s}$

wave is bounded by the nonlinear stiffness κ_{nx} as well as the linear stiffness.

It is also found from Fig. 4 that the linear stiffness κ_x plays a key role too in the dispersion characteristics in entire region. Phase velocity is increased up to 10% by the increase of the linear stiffness κ_{nx}. On the contrary to the nonlinear stiffness, the higher linear stiffness makes the A-wave faster. However, if the linear stiffness κ_x is very high in Fig. 4, the phase velocity is almost constant and insensitive to the nonlinear stiffness κ_{nx}. The dispersion curve is redrawn in Fig. 5 with respect to frequency to investigate the effect of the wave frequency on the phase velocity of the A-wave. The A-wave velocity is reduced by the use of higher frequency and approaches the Rayleigh wave velocity when the frequency goes to GHz level in Fig. 5. On the contrary it increases and asymptotes to the shear wave velocity as the frequency decreases down to KHz order. It can be deduced that this dependency of phase velocity on the linear and nonlinear stiffnesses can be used to analyze and estimate the contact state of non-welded interface such as closed cracks.

It is likely to be more practical to assume a light nonlinearity for dry contacts of engineering metals. In that case, the dispersion equations (11) and (13) reduce to eqns. (14) and (15), which are still dispersive and described in Fig. 6 as a function of frequency. Fig. 6 shows that the A-waves approach an asymptote defined by the shear wave velocity for sufficiently low frequency or high linear stiffness, and approach the Rayleigh wave velocity for high frequency or low linear stiffness. Fig. 6 also reveals that the linear stiffness can be determined by measuring the wave velocity of A-wave. If the contact interface is so tight and completely closed that the interface has the very large values of stiffness, the wave velocity of A-wave gets close to the shear wave velocity. If the contact interface is loose, the stiffness becomes small and the wave velocity is close to the Rayleigh wave velocity. Thus the dispersion curve gives a

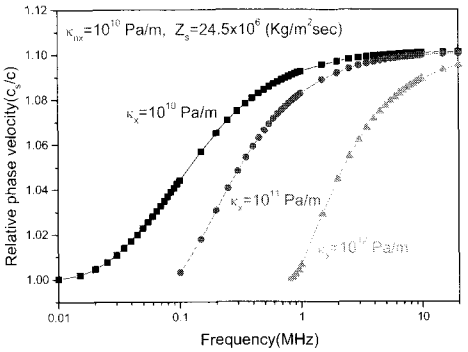

Fig. 5 Dispersion for A-wave as a function of frequency

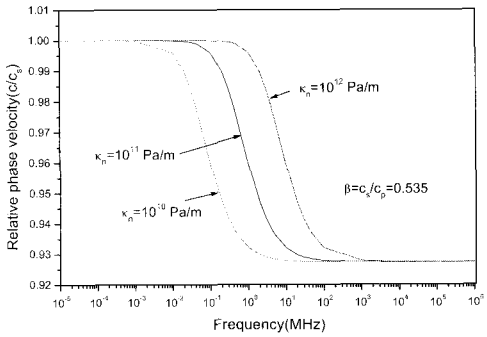

Fig. 6 Dispersion of A-wave when $\kappa_{nx}=0$

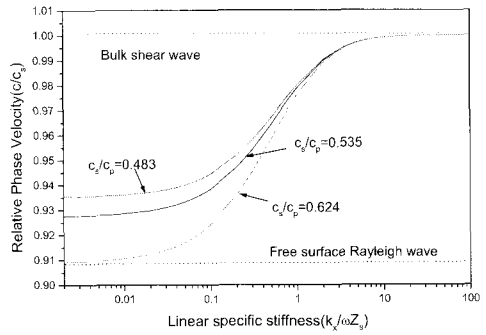

Fig. 7 Dispersion of A-wave as a function of specific linear stiffness when $\kappa_{nx}=0$

tool for estimation of the contact state of non-welded interface such as cracks or welded joints. It is plotted again in Fig. 7 in terms of linear specific shear stiffness for different values of $\beta=c_s/c_p$ representing different materials, for instance, $\beta=0.535$ for steel and $\beta=0.624$ for aluminum. In the figure, the dispersion becomes relatively weak for low β and strong for high β.

5. Conclusions

Interface waves of contact interface as generalized Rayleigh waves propagating along contact interface are demonstrated in theory based on nonlinear displacement discontinuity model. Hysteretic nonlinear model for contact interface is developed to relate discontinuous displacements with tractions on both sides of the contact interface employing the hysteretic nonlinear contact stiffness. Analytic solutions are derived to obtain the dispersion curves for the symmetric and anti-symmetric interface waves. Dispersion equations indicate that symmetric mode exists only as leaky wave and anti-symmetric mode can propagate along the interface as guided wave if the nonlinear stiffness is pure imaginary complex like viscosity. Theoretical results show that the phase velocity of the anti-symmetric wave is sensitive to contact state and changed seriously as much as 10% depending on both linear and nonlinear stiffness. It is also observed that the phase velocity of the anti-symmetric wave is bounded ranging between the shear wave velocity and the Rayleigh wave velocity when the nonlinear stiffness is neglected, It is expected that this interface waves can be applied to detect and estimate closed cracks by measuring contact stiffness or the interface waves.

Acknowledgments

This work was supported by the Korea Science and Engineering Foundation (KOSEF) grant funded by the Korea government(MOST).

References

Biwa, S., Hiraiwa, S. and Matsumoto, E. (2006) Experimental and Theoretical Study of Harmonic Generation at Contacting Interface, Ultrasonics, Vol. 44, pp. 1319–1322

Biwa, S., Suzuki, A. and Ohno, N. (2005) Evaluation of Interface Wave Velocity, Reflection Coefficients and Interfacial Stiffnesses of Contacting Surfaces, Ultrasonics, Vol. 43, pp. 495–502

Delsanto, P. P., Sigrun Hirsekorn, V. Agostini, Loparco, and Koka, A. (2002) Modeling the Propagation of Ultrasonic Waves in the Interface Region Between Two Bonded Elements, Ultrasonics, Vol. 40, pp. 605–610

Kim, J. Y., Baltazar, A., Hu, J. W., and Rokhlin, S. I. (2006) Hysteretic Iinear and Nonlinear Acoustic Responses from Pressed Interfaces, International Journal of Solids and Structures, Vol. 43, pp. 6436–6452

Kim, J. Y., Baltazar, A. and Rokhlin, S. I. (2004) Ultrasonic Assessment of Rough Surface Contact Between Solids from Elasto-Plastic Loading-Unloading Hysteresis Cycle, Journal of the Mechanics and Physics of Solids, Vol. 52, pp. 1911-1934

Nihei, K. T, Gu, B., Myer, L. R., L. J. Pyrak-Nolte and Cook, N. G. (1995) Elastic Interface Wave Propagation Along a Fracture, International Congress on Rock Mechanics, Vol. 3, pp. 1151-1157

Pyrak-Nolte, L. J. and Cook, N. G. W. (1987) Elastic Interface Waves Along a Fracture, Geophys. Res. Lett. 14, pp. 1107–1110

Pyrak-Nolte, L. J., Xu, J. and Hayley, G. M. (1992) Elastic Interface Waves Along a Fracture: Theory and Experiment, Rock Mechanics Proceedings of the 33rd U.S. Symposium. New Mexico, USA, pp. 999-1007

Roy, S. and Pyrak-Nolte, L. J. (1995) Interface Waves Propagating Along Tensile Fractures in Dolomite, Geophys. Res. Lett. 22 (20), pp. 2773–2776